JOURNAL OF NANO- AND ELECTRONIC PHYSICS
Vol. **17** No 1, 01003(8pp) (2025)

ЖУРНАЛ НАНО- ТА ЕЛЕКТРОННОЇ ФІЗИКИ
Том **17** № 1, 01003(8cc) (2025)

OPEN ACCESS

REGULAR ARTICLE

Fabrication and Characterization of Nanostructured NiO and NiO:Cu Thin Films at Varied Copper Concentrations

Y. Boussida[1,2,*], Y. Aoun[1,2], N. Djilani[1,2], A. Djelloul[3,†]

[1] *Mechanical Department, Faculty of Technology, University of El-Oued, El-Oued 39000, Algeria*
[2] *Arid Zone Renewable Energy Development Unit, University of El-Oued, El-Oued 39000, Algeria*
[3] *Centre de Recherche en Technologie des Semi-Conducteurs pour l'Energétique 'CRTSE', 02 Bd Frantz Fanon, BP 140, 7 Merveilles, Alger, Algérie*

(Received 03 November 2024; revised manuscript received 14 February 2025; published online 27 February 2025)

Nickel oxide (NiO) is a semiconductor with a face-centered cubic (*fcc*) crystalline structure. Due to its wide band gap, high transparency, and porous surface morphology, NiO exhibits high performance in various electronic and optoelectronic devices. For this reason, metal-doped NiO thin films have recently attracted the attention of researchers. In this study, NiO and copper-doped (Cu-doped) NiO thin films were deposited on glass substrates at a temperature of 420 °C using a simple and cost-effective spray pyrolysis technique. The amount of Cu doping was varied at different concentrations (0.5 %, 1.5 %, 3 %, and 6 % by weight). The structure, morphology, chemical composition, optical properties and 3D topography analysis of the deposited films were investigated. X-ray diffraction analysis shows that both NiO and Cu-doped NiO films exhibit an *fcc* structure with a dominant (111) peak. The crystallite size decreases from 26.78 to 18.15 nm with Cu doping. Surface morphology was examined using a scanning electron microscope (SEM). In the SEM images, all samples show the formation of small aggregates of irregular particles on the heterogeneous surface. The chemical composition and stoichiometry of the deposited thin films were confirmed by energy-dispersive X-ray spectroscopy (EDS). The optical band gap (E_g) of the deposited films was determined through absorption measurements, demonstrating a decrease with increasing concentrations of Cu dopant.

Keywords: Nickel oxide thin films, Cu-doped NiO, Spray pyrolysis technique, X-ray diffraction, 3D surface topography.

DOI: 10.21272/jnep.17(1).01003

PACS numbers: 73.61.Jc, 81.15.Rs, 07.85.Nc, 68.37.Ps

1. INTRODUCTION

In recent years, there has been significant research conducted on transparent conducting oxides (TCOs) owing to their desirable characteristics, such as high optical transparency and effective electrical conductivity. Commonly utilized TCOs include tin oxide (SnO2), indium tin oxide (ITO), and zinc oxide (ZnO), which find widespread applications in optoelectronic devices [1-3]. These TCOs are categorized as *n*-type semiconductors, and there is a growing interest in discovering new versatile *p*-type TCOs. Among many oxide thin films, nickel oxide (NiO) is one of the most interesting candidates in this class due to its high bandgap from 1.5 to 3 eV, *p*-type conductivity, and remarkable morphological, structural, electrical, and optical properties. Several deposition techniques can be used to prepare NiO thin films, such as DC magnetron sputtering [4, 5], RF magnetron sputtering [3, 6], thermal evaporation [7], beam evaporation [8], vacuum evaporation [9], pulsed laser deposition [10], chemical vapor deposition [11], anodic deposition [12], electrochemical deposition [13], electroless bath deposition [14], chemical bath deposition [15], sol-gel [16, 17], and spray pyrolysis [18, 19]. The latter technique is considered the most suitable for obtaining dense and porous NiO thin films. Moreover, it has many advantages such as simplicity, low cost, safety, no high vacuum requirements, and is also helpful for large-area applications [20, 21]. NiO films are used in many film applications, such as organic light-emitting diodes (OLEDs) [20], electronic switching and information displays [22], liquid crystal displays (LCDs) [23], chemical sensors [24], and solar cells [19].

Nickel oxide, known for its exceptional chemical stability and distinctive optical, electrical, and magnetic properties, has garnered considerable attention. Nickel oxide (NiO) is an impressive semiconductor material with a partially transparent nature, exhibiting a cubic rock salt-like structure characterized by octahedral Ni_2^+ and O_2^- sites [25].

* Correspondence e-mail: yousra-boussida@univ-eloued.dz
† djelloulcrtse@gmail.com

Cite this article as: Y. Boussida et al., *J. Nano- Electron. Phys.* 17 No 1, 01003 (2025) https://doi.org/10.21272/jnep.17(1).01003

It possesses a considerable optical band-gap of 3.6 eV and demonstrates favorable thermoelectric and catalytic properties [19, 26]. Typically, NiO deviates from stoichiometry, meaning that the NiO ratio varies from the ideal 1:1 composition. The introduction of dopant metals such as La, Cd, Mg, K, and Cu can significantly influence the material's properties. However, there has been limited research conducted on Cu-doped NiO thin films in the past [27]. To proceed, a concise overview of the previous studies available in the literature concerning Cu-doped NiO thin films. Chen et al. [28] utilized the radio frequency magnetron sputtering method to produce NiO–Cu composite films on a glass substrate. This involved sputtering NiO–Cu composite targets in an argon atmosphere at room temperature. The films deposited had varying concentrations of Cu, ranging from 2.29 % to 18.17 %. Analysis of the films using Hall measurement indicated p-type conduction. The researchers hypothesized that the substitution of Ni^{+}_{2} ions (0.78 Å) with Cu^{+} ions (0.96 Å) within the NiO lattice contributed to p-type conduction by increasing carrier concentration, resulting in decreased resistivity of the films. Additionally, as the Cu content increased within the range of 2.29 % to 18.17 %, the transmittance of the NiO–Cu composite films exhibited a consistent de-crease. X-ray diffraction analysis of the thin films only showed NiO peaks, with no presence of Cu peaks. The intensity of the diffraction peaks diminished as the Cu concentration increased, indicating a deterioration in the crystallinity of the films, particularly when surpassing 6.97 % Cu. Aftab et al. [29] expanded upon the previous investigations conducted on NiO:Cu thin films produced on pre-heated glass substrates (at 410°C) through spray pyrolysis technique. The XRD analysis revealed that the polycrystalline thin films exhibited a cubic structure with a preferential orientation along the (111) and (200) planes. The crystallite size (varying from 94 to 27 nm) decreased while the stacking fault probability (0.014 – 0.147) and the lattice strain (0.0014 – 0.0113) increased as the Cu/Ni ratio increased. However, the specific values of the lattice strain and crystal-lite size for a given Cu/Ni ratio relied on the chosen analytical model. As the Cu/Ni ratio increased, both the surface roughness and the density of surface pores in the films decreased. Additionally, Dawood et al. [30] carried out a study to investigate the effects of Cu doping on the optical properties of NiO thin films. These films, which had a thickness of around 350 ± 20 nm, were fabricated on microscopic glass substrates using a spray pyrolysis method. The doping levels that were utilized were 2 % and 4 % copper, and the substrate temperature was kept at 400 °C. Transmittance and absorbance spectra were taken at the wavelength range 380 – 900 nm. With an increase in the concentration of Cu in the NiO thin films, the direct band gap (varying from 3.10 to 2.90 eV) and dispersion parameters de-creased, while the Urbach energy increased from 0.584 to 0.671 eV. This study focuses on the examination of Cu-doped NiO films using the cost-effective spray pyrolysis method. Consequently, it is of interest to explore the impact of varying Cu concentrations on the physical characteristics of both undoped and copper-doped thin films of NiO. The physical properties encompassing structural, morphological and optical properties of the films are analyzed through techniques such as X-Ray Diffraction (XRD), Scanning electron microscopy (SEM), Energy dispersive X-ray spectroscopy (EDS), Atomic force electron microscopy (AFM), Ultraviolet–visible spectrophotometry (Uv-Vis) and Photoluminescence (PL) spectroscopy. It is anticipated that the introduction of Cu will enhance the conductivity and transparency of the NiO thin films.

2. EXPERIMENTAL DETAILS

2.1 Materials

To fabricate the pure NiO and NiO/Cu thin films, nickel chloride hexahydrate ($NiCl_2{\cdot}6H_2O$) was employed as the initial precursor, while copper (II) nitrate trihydrate $Cu(NO_3)_2{\cdot}3H_2O$ was chosen as the doping agent. All the necessary pure analytical materials were obtained from Sigma Aldrich and used without requiring additional purification.

2.2 Thin Film Deposition

Firstly, a solution of 0.1 M $NiCl_2{\cdot}6H_2O$ was prepared by dissolving it in double-distilled water. When creating copper-doped films at varying concentrations (0.5 %, 1.5 %, 3 %, and 6 % by weight), copper nitrate was mixed with the 0.15 M $NiCl_2{\cdot}6H_2O$ precursor solution. Soapy water and ethanol were used to wash and sonicate NiO:Cu thin films to remove impurities from the substrate. After 120 minutes of stirring at 60 °C, the solution was clear and transparent. The solutions obtained were applied onto glass substrates measuring 30 mm × 7.5 mm × 1 mm and then heated using the spray pyrolysis method. Heating the substrates was done using the solar cell method. This letter was crafted in our research facility. In order to obtain high-quality thin films, the spray parameters were fine-tuned. This involved setting the flow rate to 1 ml/min, keeping the substrate-nozzle distance at 5 cm, using a compressed air pressure of 1.5 kg/cm^2, and ensuring the substrate temperature stayed constant at 420 °C.

2.3 Films Characterization

The film surface morphology was analyzed by Atomic Force Microscope (AFM).

Different methods were employed to study undoped NiO and NiO/Cu films. The characterization of the obtained thin films was performed using X-ray diffraction with a Bruker (D8 Advance model) diffractometer. The X-ray diffraction analysis was conducted at room temperature, scanning from 10 to 80° at a rate of 0.03° s^{-1}, using CuKa radiation with a wavelength of 1.5406 Å. The size of the NiO and Cu/NiO crystallites in the X-ray diffraction pattern was estimated using the Debye–Scherrer's Eq. 1 [31]:

$$D = N\lambda / (\beta \cos\theta). \quad (1)$$

Were D represent the size of the crystallite, N denotes a numerical coefficient, λ represents the X-ray's wavelength, β represents the full-width half-maximum, and θ refers to the diffraction angle. The fundamental chemical composition and morphology were examined using a JEOL-JSM 5800 scanning electron microscope (SEM) coupled with an energy dispersive X-ray spectroscopy (EDS) system.

Optical transmission spectra and absorbance of the films were investigated using UV-vis equipment (Spectrum SP-UV300SRP) operating within the wavelength range of 300 – 900 nm. The Tauc and Menth Eq. (2) were employed to calculate the band-gap values [32]:

$$\alpha h\upsilon = A\left(h\upsilon - E_g\right)^{\eta}. \qquad (2)$$

Where α represents the absorptivity, h denotes Planck's constant, υ represents the frequency of radiation, E_g represents the visual indirect band-gap, A stands for the constant of proportionality, and η indicates the type of optical transition resulting from photon absorption. To determine the 3D surface topography and surface roughness, a Tencor P-7 mechanical profilometer was utilized under ambient atmospheric conditions and at room temperature. The measurements were conducted using the 2-bar technique with filter modification (Gaussian filter, 0.800 m cut-off, accounting for edge effects).

3. RESULT AND DISCUSSION

3.1 XRD Analysis

The XRD patterns of undoped NiO and Cu-doped NiO thin films (0.5 %, 1.5 %, 3 %, and 6 %) on glass substrates are shown in Fig. 1. This figure depicts the correlation between intensity (a.u.) and the 2θ angle position (in degrees). By eliminating background noise from the diffraction angles, the spectra were presented within the range of 20° to 80°. Among all the thin films created, only one diffraction peak was observed at a 2θ value of 37.36°, corresponding to the (111) plane of the cubic-structured crystalline NiO (Fig. 1). This observation aligns with the JCPDS card No.47-1049, indicating the absence of significant peaks associated with copper (Cu) or copper oxide (CuO). Consequently, this indicates the absence of secondary phases and the successful incorporation of Cu atoms into the NiO lattice at the Ni sites. The observed peak broadening could be due to the increased amorphous nature resulting from the addition of copper doping. Initially, the peak intensity increases with increasing Cu concentration up to 3 wt % but then gradually decreases at higher Cu concentrations (specifically, 6 wt %). The decrease in the intensity of the diffraction peak can be attributed to the increased concentration of point defects.

3.2 SEM and EDS Analysis

SEM images of NiO thin films with varying Cu concentrations (0.5, 1.5, 3, and 6 wt %) revealed the formation of small, irregular particle aggregates on the heterogeneous surface, indicating that increasing Cu concentration significantly impacts the film's surface structure. This particle growth can be attributed to rapid diffusion and reduced activation energies associated with higher Cu concentrations (Fig. 3).

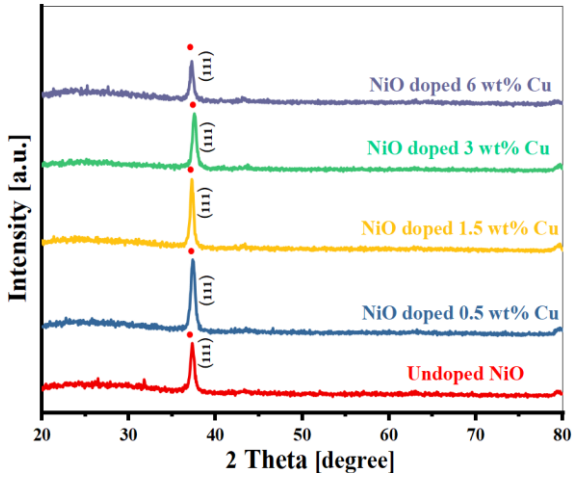

Fig. 1 – The XRD patterns of undoped NiO thin films and Cu-doped NiO thin films (0.5 %, 1.5 %, 3 %, and 6 %)

EDS analysis was used to examine the chemical composition of the Cu/NiO film, revealing peaks corresponding to Ni, Si, and O elements (Fig. 3). The presence of a heterogeneous surface promotes increased adsorption of methylene blue and enhances the films' photocatalytic efficiency. Fig. 2(a-e) demonstrates that as the concentration increased, the surface of the films exhibited more grains, with their size expanding accordingly, resulting in a rougher surface, as confirmed by the roughness data (Table 1).

3.3 AFM Analysis

The 3D surface topography illustrates the surface roughness gradients for the NiO/Cu thin films displayed in Fig. 4. The findings indicate that the surface roughness and heterogeneity increase with higher concentrations of Cu (from 0.5 to 6 wt %). The Rq values for all films ranged from 0.0567 to 0.183 μm, as shown in Table 1. At 6 wt %, tenorite thin film had a surface roughness of 0.183 nm, which increased the film's specific surface area. The highest peak heights (Rp) observed on the surfaces of the NiO thin film and NiO/Cu thin film were 0.438 μm, 0.275 μm, 0.388 μm, 0.713 μm, and 0.762 μm at concentrations of 0 g/ml, 0.5 g/ml, 1.5 g/ml, 3 g/ml, and 6 g/ml, respectively. As indicated in Table 1, surface roughness increases with the thickness of the film, leading to a more heterogeneous NiO/Cu film surface, as depicted in Fig. 4.

Hence, the NiO/Cu film produced at a 0.5 wt% exhibited the lowest surface roughness (R_q) value of 0.128 μm, indicating a homogeneous distribution of NiO/Cu particles on the film surface. Conversely, the roughness parameters of the 5 wt% film were higher compared to those of the pure NiO film.

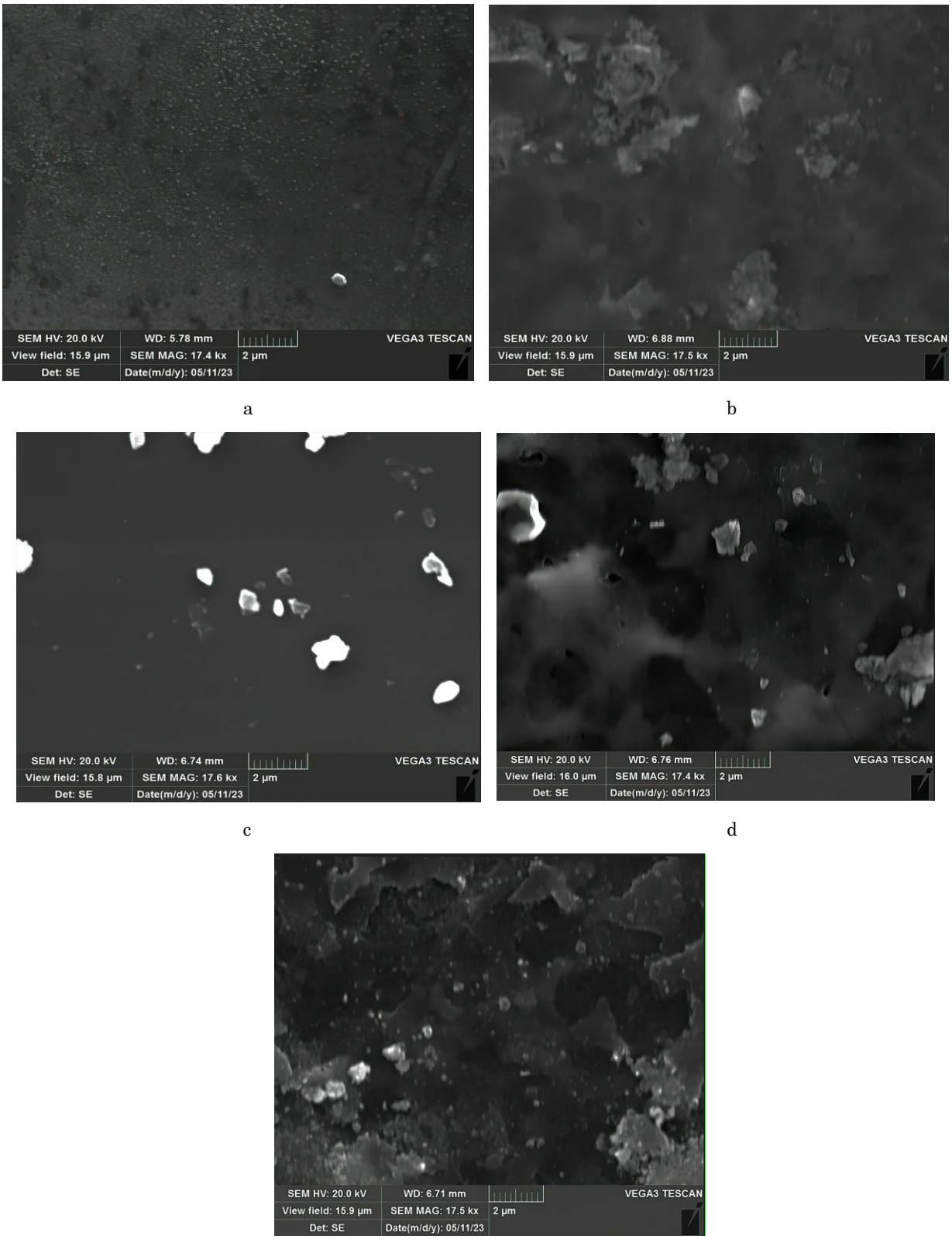

Fig. 2 – SEM micrographs of: (a) undoped NiO, (b) NiO: 0.5 % Cu, (c) NiO: 1.5 % Cu, (d) NiO: 3 % Cu and (e) NiO: 6 % Cu thin films

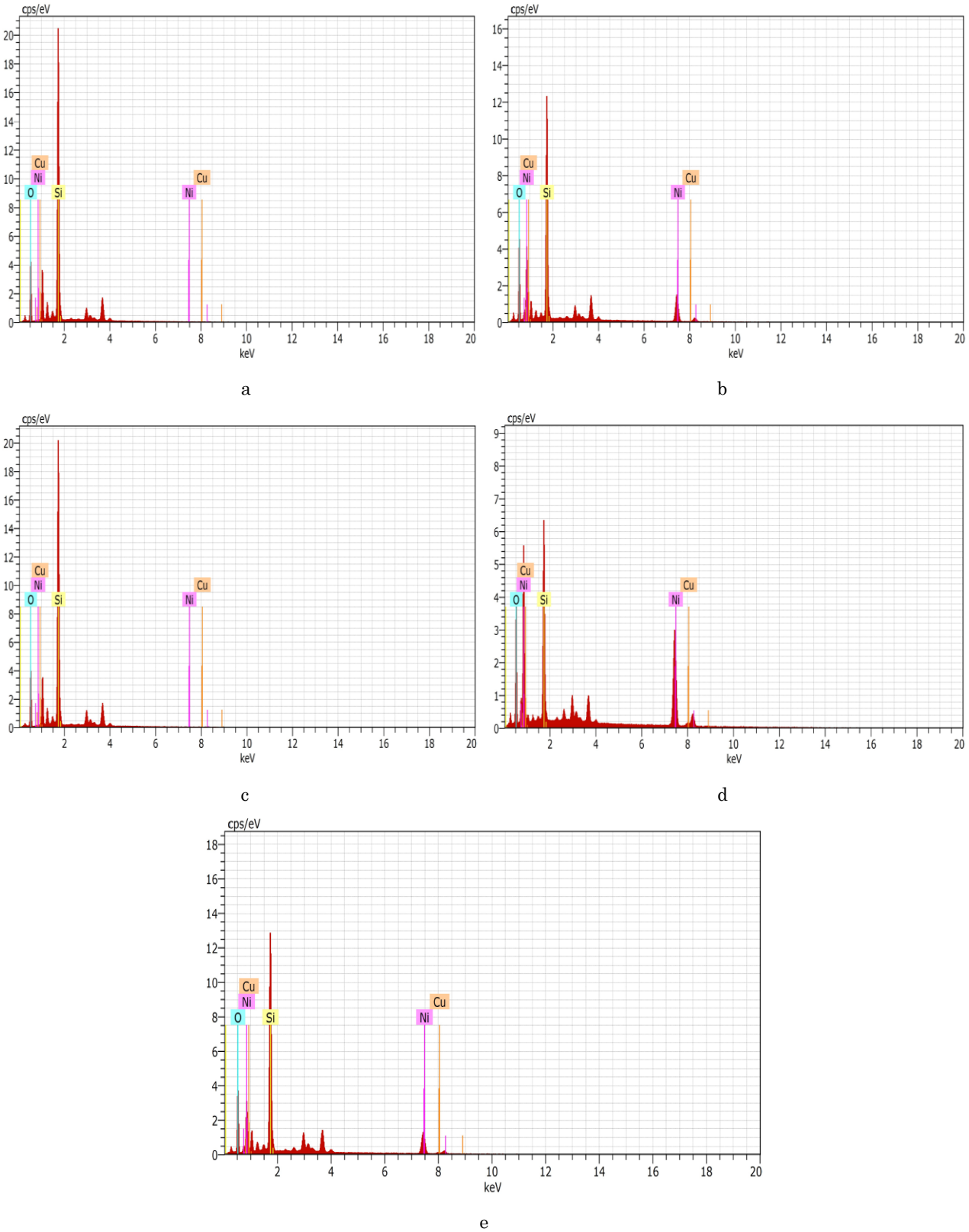

Fig. 3 – EDS composition analysis of: (a) undoped NiO, (b) NiO: 0.5 % Cu, (c) NiO: 1.5 % Cu, (d) NiO: 3 % Cu and (e) NiO: 6 % Cu thin films

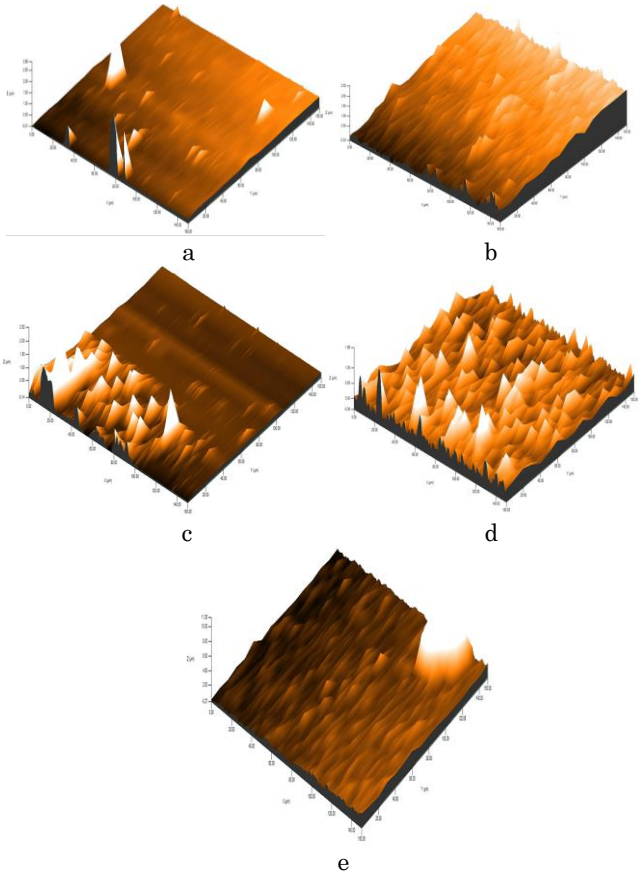

Fig. 4 – The 3D AFM images of: (a) undoped NiO, (b) NiO: 0.5% Cu, (c) NiO: 1.5% Cu, (d) NiO: 3% Cu and (e) NiO: 6% Cu thin films

Furthermore, these roughness parameters increased as the Cu doping concentration increased, with the surface roughness reaching 0.183 μm at 6 wt% of Cu. This significant change in surface homogeneity and roughness, as well as the morphological structure depicted in Fig. 3, can be explained by the assumption that higher concentrations of Cu on the NiO surface induce instability with dynamic effects, leading to the formation of smaller and larger aggregations in the film's particle distribution.

3.4 Optical Properties

NiO thin films exhibit a wide range of transparency in the visible region. In Fig. 5(a), the transmission spectra of NiO films demonstrate varying transmittance rates, on average ranging from 53 % to 29 % at a wave-length of (300 – 900) nm. The impact of Cu concentration (0.5, 1.5, 3, and 6 wt %) on transmittance is shown, revealing the influence of oxygen content (43.47, 34.66, 42.41, 24.60, and 31.88 C norm. wt. %) and film thick-ness (217.6, 227, 247.3, 284.7, and 558.2 nm) on transmittance values of 53 %, 48 %, 45 %, 41 %, and 29 %, respectively. Notably, higher Cu/NiO film thickness results in a significant reduction in optical transmittance. The Tauc plot in Fig. 5(b) illustrates the changes in the direct bandgap (E_g) of NiO films. Table 1 shows that the

Table 1 – Results report

Samples	Thickness [nm]	Grain size [nm]	Transmittance [%]	Band Gap [eV]	Surface Roughness Rq [μm]
Undoped NiO	217.6	26.78	53	3.2	0.0567
0.5 wt % Cu	227.1	19.02	48	2.9	0.128
1.5 wt % Cu	247.3	21.72	45	3.07	0.0835
3 wt % Cu	284.7	18.15	41.6	3.03	0.178
6 wt % Cu	558.2	21.72	29	2.8	0.183

direct bandgap values (ranging from 2.8 to 3.2 eV) remain unaffected by Cu concentration (0 to 6 wt %), crystal size, and film thickness. However, increasing Cu concentration leads to changes in film thickness, structure, and morphology of Cu/NiO films. Moreover, Fig. 5b depicts the decrease in the bandgap by an increase in the concentration of Cu. Fig. 5c illustrates the relationship between the optical bandgap energy and the Cu concentration (wt. %). The investigation revealed a discernible decrease in the optical bandgap as the Cu concentration increased from 0.5 to 1.5 wt. %. This phenomenon strongly suggests the formation of Cu nanoparticles on the NiO Films.

Moreover, the bandgap energy of the NiO thin films was observed to vary between 2.8 and 3.2 eV, a range that closely aligns with the known Eg value of bulk NiO (3.6 – 4 eV). This observation indicates a consistent behavior between the thin films and the bulk material in terms of their optical bandgap characteristics.

4. CONCLUSION

In conclusion, this study focused on the production of NiO semiconductor films using the pyrolysis technique with different concentrations of Cu doping (0.5, 1.5, 3, and 6 wt%). The objective was to investigate the impact of Cu doping on the physical and chemical properties of NiO films. The analysis involved several techniques such as XRD, SEM, EDS, AFM and UV-Vis. The results showed that the deposited Cu/NiO thin films exhibited a crystalline characteristic and possessed a cubic phase structure, as confirmed by the XRD analysis. Additionally, the optical bandgap (E_g) of the films was measured, and it was observed that the E_g decreased with an increase in the concentration of Cu dopants. This study provides valuable insights into the fabrication of NiO semiconductor films and highlights the influence of Cu doping on their physical and chemical properties. The findings contribute to the understanding of semiconductor film manufacturing processes and may have implications for the development of improved and more efficient fabrication techniques in diverse applications.

ACKNOWLEDGEMENTS

The authors would like to thank the General Directorate for Scientific Research and Technological Development (DGRST).

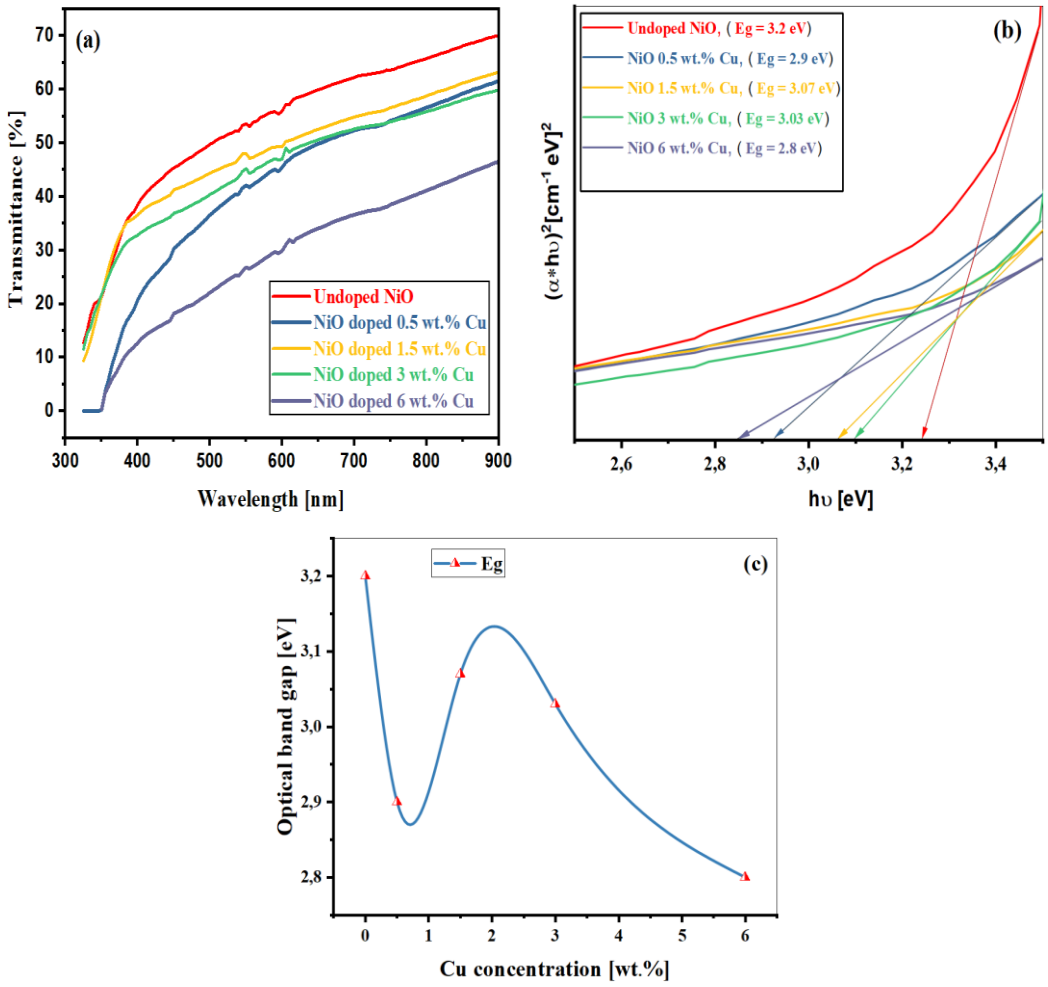

Fig. 5 – (a) The optical transmission of thin films of undoped NiO and Cu-doped NiO (0.5 %, 1.5 %, 3 %, and 6 %), (b) Energy band gap of NiO pure and Cu-doped NiO (0.5 %, 1.5 %, 3 %, and 6 %), (c) The variations of optical bandgap vs Cu concentration

REFERENCES

1. R.K. Gupta, K. Ghosh, P.K. Kahol, *Mater. Lett.* **64** No 18, 2022 (2010).
2. H. Hosono, *Thin Solid Films* **515** No 15, 6000 (2007).
3. S. Nandy, U.N. Maiti, C.K. Ghosh, K.K. Chattopadhyay, *J. Phys.: Condens. Matter* **21** No 11, 115804 (2009).
4. Y. Zhou, D. Gu, Y. Geng, F. Gan. *Mater. Sci. Eng.: B* **135** No 2, 125 (2006).
5. J.A. Glasscock, D. Gu, Y. Geng, F. Gan, *J. Phys. Chem. C* **111** No 44, 16477 (2007).
6. Y.M. Lu, W.S. Hwang, J.S. Yang, H.C. Chuang. *Thin Solid Films* **420**, 54 (2002).
7. D. Suthar, R. Sharma, A. Sharma, Himanshu, A. Thakur, M.D. Kannan, M.S. Dhaka, *J. Alloy. Compd.* **918**, 165756 (2022).
8. K. Ganga Reddy, P. Nagaraju, G.L.N. Reddy, P. Ghosal, M.V. Ramana Reddy, *Sensor. Actuat. A: Phys.* **346**, 113876 (2022).
9. D. Dastan, K. Shan, A. Jafari, T. Marszalek, M.K.A. Mohammed, L. Tao, Z. Shi, Y. Chen, X.-T. Yin, N.D. Alharbi, F. Gity, S. Asgary, M. Hatamvand, L. Ansari, *Mater. Sci. Semicond. Proc.* **154**, 107232 (2023).
10. J. Som, J. Choi, H. Zhang, N.R. Mucha, S. Fialkova, K. Mensah-Darkwa, J. Suntivich, R.K. Gupta, D. Kumar, *Mater. Sci. Eng. B* **280**, 115711 (2022).
11. M. Yang, H. Zhu, Y. Zheng, C. Zhang, G. Luo, Q. Xu, Q. Li, S. Zhang, T. Goto, R. Tu, *RSC Adv.* **12** No 17, 10496 (2022).
12. K.H. Parmar, V. Manjunath, S. Bimli, P.R. Chikate, R.A. Patil, Y.-R. Ma, R.S. Devan, *Chinese J. Phys.* **77**, 143 (2022).
13. J. El Nady, A. Shokry, M. Khalil, S. Ebrahim, A.M. Elshaer, M. Anas, *Sci. Rep.* **12** No 1, 3611 (2022).
14. I. Schapiro, M. Shandalov, N. Maman, V. Ezersky, Y. Golan, E. Yahel, *Cryst. Res. Technol.* **57** No 8, 2100194 (2022).
15. L. Li, W. Shen, C. Yang, Y. Dou, X. Zhu, Y. Dong, J. Zhao, J. Xiao, F. Huang, Y.-B. Cheng, J. Zhong, *J. Mater. Sci. Technol.* **133**, 145 (2023).
16. E. Benrezgua, B. Deghfel, A. Zoukel, W.J. Basirun, R. Amari, A. Boukhari, M.K. Yaakob, S. Kheawhom, A.A. Mohamad, *J. Molec. Struct.* **1267**, 133639 (2022).
17. N. Aswathy, J. Varghese, S.R. Nair, R. Vinod Kumar, *Mater. Chem. Phys.* **282**, 125916 (2022).

18. I.L.P. Raj, S. Valanarasu, S. Vinoth, N. Chidhambaram, R.S. Rimal Isaac, M. Ubaidullah, S.F. Shaikh, B. Pandit, *Sensor. Actuat. A: Phys.* **333**, 113242 (2022).
19. V.A. Owoeye, S.A. Adewinbi, A.O. Salau, A.N. Orelusi, A.E. Adeoye, A.T. Akindadelo. *Heliyon* **9** No 1, e13023 (2023).
20. V.H. López-Lugo, M. García-Hipólito, A. Rodríguez-Gómez, J.C. Alonso-Huitrón, *Nanomaterials* **13** No 1, 197 (2023).
21. V. Ganesh, H.S. Akkera, Y. Bitla, L. Haritha, S. Al Faify, I.S. Yahia, *Physica B: Condens. Matter* **635,** 413786 (2022).
22. I.L.P. Raj, S. Valanarasu, A. Asuntha, R.S. Rimal Isaac, M. Shkir, H. Algarni, S. Al Faify, *J. Mater. Sci.: Mater. Electron.* **33**, 11753 (2022).
23. N. Katariya, B. Singh, A. Saxena, V. Ganesan. *Macromolec. Symposia* **407** No 1, (2023).
24. A. Moumen, G.C. Kumarage, E. Comini, *Sensors* **22** No 4, 1359 (2022).
25. Q. Zhao, C. Fang, F. Tie, W. Luo, Y. Peng, F. Huang, Z. Ku, Y.-B. Cheng. *Mater. Sci. Semicond. Proc.* **148**, 106839 (2022).
26. M. Obaida, A.M. Fathi, I. Moussa, H.H. Afify, *J. Mater. Res.* **37** No 14, 2282 (2022).
27. A. Javadian, M. Fadavieslam, *J. Mater. Sci.: Mater. Electron.* **33** No 30, 23362 (2022).
28. S.C. Chen, T.Y. Kuo, Y.C. Lin, H.C. Lin. *Thin Solid Films* **519** No 15, 4944 (2011).
29. M. Aftab, M.Z. Butt, D. Ali, F. Bashir, T.M. Khan, *Opt. Mater.* **119** 111369 (2021).
30. M.O. Dawood, *Int. Lett. Chem., Phys. Astron.* **48**, 138 (2015).
31. M.A. Bouacheria, A. Djelloul, M. Adnane, Y. Larbah, L. Benharrat, *J. Inorg. Organometal. Polym. Mater.* **32**, 2737 (2022).
32. J. Tauc, A. Menth, *J. Non-Cryst. Solid* **8–10**, 569 (1972).

Виготовлення та характеристика наноструктурованих тонких плівок NiO та NiO:Cu при різних концентраціях міді

Y. Boussida[1,2], Y. Aoun[1,2], N. Djilani[1,2], A. Djelloul[3]

[1] *Mechanical Department, Faculty of Technology, University of El-Oued, El-Oued 39000, Algeria*
[2] *Arid Zone Renewable Energy Development Unit, University of El-Oued, El-Oued 39000, Algeria*
[3] *Centre de Recherche en Technologie des Semi-Conducteurs pour l'Energétique 'CRTSE', 02 Bd Frantz Fanon, BP 140, 7 Merveilles, Alger, Algérie*

Оксид нікелю (NiO) – напівпровідник із гранецентрованою кубічною (ГЦК) кристалічною структурою. Завдяки широкій забороненій зоні, високій прозорості та морфології пористої поверхні NiO демонструє високу продуктивність у різних електронних та оптоелектронних пристроях. З цієї причини нещодавно увагу дослідників привернули леговані металом тонкі плівки NiO. У даній роботі NiO та леговані міддю (Cu-леговані) тонкі плівки NiO були нанесені на скляні підкладки при температурі 420 °C за допомогою простої та економічно ефективної техніки розпилювального піролізу. Кількість легуючої міді змінювалася при різних концентраціях (0,5 %, 1,5 %, 3 % і 6 % за масою). Досліджено структуру, морфологію, хімічний склад, оптичні властивості та 3D топографічний аналіз нанесених плівок. Рентгеноструктурний аналіз показує, що плівки NiO і NiO, леговані Cu, демонструють ГЦК структуру з домінуючим піком (111). Розмір кристалітів зменшується з 26,78 до 18,15 нм при легуванні Cu. Морфологію поверхні досліджували за допомогою скануючого електронного мікроскопа (SEM). На SEM-зображеннях усі зразки показують утворення невеликих агрегатів неправильних частинок на неоднорідній поверхні. Хімічний склад і стехіометрія нанесених тонких плівок були підтверджені методом енергодисперсійної рентгенівської спектроскопії (EPC). Ширина забороненої зони (Eg) осаджених плівок була визначена за допомогою вимірювань поглинання, що демонструє зменшення зі збільшенням концентрації легуючої домішки Cu.

Ключові слова: Тонкі плівки оксиду нікелю, Легований Cu NiO, Метод розпилювального піролізу, Рентгенівська дифракція, 3D рельєф поверхні.